CPT-based design of pile foundations in sand and clay: perspectives

Venkata Abhishek Sakleshpur[#], *Monica* Prezzi, and *Rodrigo* Salgado

Purdue University, Lyles School of Civil Engineering, West Lafayette, IN, USA
[#]*Corresponding author: vsaklesh@purdue.edu*

ABSTRACT

This paper provides some perspectives and guidance for the design of pile foundations in sand and clay using cone penetration test (CPT) results. A key variable in the estimation of the limit unit shaft resistance q_{sL} of piles in sand is the critical-state interface friction angle δ_c, which is a function of the critical-state friction angle ϕ_c of the sand. In the absence of direct shear or triaxial compression test results, which is often the case for routine infrastructure projects, engineers typically assume a conservative value for ϕ_c in pile design. In addition, effective stress-based methods for estimation of q_{sL} of driven piles in clay rely on the residual interface friction angle δ_r, among other variables; however, in these methods, δ_r does not vary with the normal effective stress on the pile operative at the time of shearing. In this paper, we present relationships and approaches to address these issues. Finally, a relationship between the cone resistance q_c and the corrected standard penetration test (SPT) blow count N_{60} was also developed so that engineers may obtain an estimate of q_c for use in a CPT-based design method when only SPT blow counts are available for a site.

Keywords: Cone penetration test; pile foundation; sand; clay.

1. Introduction

A pile derives its load-carrying capacity via two mechanisms: (1) shaft resistance, resulting from friction along the pile shaft with the surrounding soil, and (2) base resistance, which is the compressive resistance at the contact of the pile base with the underlying soil. The ultimate load capacity Q_{ult} of an axially loaded pile, net of the pile weight W_{pile}, is equal to the sum of the limit shaft capacity Q_{sL} and the ultimate base capacity $Q_{b,ult}$ of the pile (Salgado 2022):

$$Q_{ult} + W_{\text{pile}} = Q_{sL} + Q_{b,ult} = \sum_{i=1}^{n} q_{sLi} A_{si} + q_{b,ult} A_b \tag{1}$$

where q_{sLi} = limit unit shaft resistance of the pile segment in contact with layer i, A_{si} = circumferential area of the pile shaft interfacing with layer i, n = number of soil layers in contact with the pile shaft, $q_{b,ult}$ = ultimate unit base resistance, and A_b = area of the pile base.

1.1. Shaft resistance of piles in sand

The critical-state friction angle ϕ_c is an important parameter in the design of pile foundations in sand. For example, the limit unit shaft resistance q_{sL} of a pile installed in sand and subjected to an axial, compressive load is given by (Salgado 2022):

$$q_{sL} = K \sigma'_{v0} \tan \delta_c \tag{2}$$

where $K = \sigma'_h/\sigma'_{v0}$, σ'_h = horizontal (normal) effective stress on the pile shaft operative at the time the pile reaches an ultimate limit state, σ'_{v0} = initial vertical effective stress before pile installation, and δ_c = pile-soil critical-state interface friction angle; all at the depth where q_{sL} is to be calculated.

In simple terms, the value of K for a sand element in contact with the pile shaft depends on the tendency of that element to either contract or dilate during shearing (Loukidis and Salgado 2008). This mechanism, in the case of nondisplacement piles (drilled shafts), for example, depends on the relative density D_R of the sand and the level of confining stress (Han et al. 2017a). The relative density D_R of sand at a given depth below the ground surface can be estimated from the cone resistance q_c if the values of σ'_{h0} (= $K_0\sigma'_{v0}$) and ϕ_c are known; σ'_{h0} = initial horizontal effective stress at the depth being considered, and K_0 = coefficient of lateral earth pressure at-rest (Salgado and Prezzi 2007).

The value of δ_c can be determined from the results of direct interface shear tests performed by shearing a sand sample against the surface of the material used to fabricate the pile (Han et al. 2018; Tehrani et al. 2016; Tovar-Valencia et al. 2018). In pile design, δ_c has been expressed as a function of ϕ_c because of the large shear strains that develop along the pile shaft at ultimate load levels, with the consequence that a sand element in contact with the pile shaft is at critical state (Basu and Salgado 2012; Foye et al. 2009; Han et al. 2017b, 2019; Sakleshpur et al. 2021a, 2021b; Salgado 2022). The value of δ_c/ϕ_c is typically equal to 1.0 for cast-in-place concrete piles (drilled shafts) and 0.95 for precast concrete piles in sand. For steel piles, the value of δ_c/ϕ_c depends on the surface roughness of the pile and the particle size and gradation of the sand (Han et al. 2018). In the absence of direct shear or triaxial compression test results, which is often the case for routine infrastructure projects, engineers typically assume a conservative value for ϕ_c in pile design. In section 2 of the paper, we present a

relationship to estimate the value of ϕ_c as a function of particle size, gradation, and morphology of the sand.

1.2. Shaft resistance of piles in clay

For piles in clay, both total stress analysis (α-approach) and effective stress analysis (β-approach) can be done for calculation of the pile shaft resistance. In an effective stress analysis, the limit unit shaft resistance q_{sL} of a pile installed in clay and subjected to an axial, compressive load is given by (Salgado 2006, 2022):

$$q_{sL} = \sigma'_{hds} \tan\delta_r \tag{3}$$

where σ'_{hds} = horizontal (normal) effective stress mobilized between the pile shaft and the disturbed soil surrounding the pile during loading, and δ_r = pile-soil residual interface friction angle; all at the depth where q_{sL} is to be calculated.

Cone penetration test (CPT)-based methods for driven piles in clay, such as the Imperial College Pile Design Method (ICPDM) (Jardine et al. 2005) and the University of Western Australia Pile Design Method (UWAPDM) (Lehane et al. 2013), have expressions for q_{sL} of the form similar to that of Eq. (3), such that σ'_{hds} may be calculated using:

$$\sigma'_{hds} = 0.8K\sigma'_{v0} \tag{4}$$

$$K = \left[2.2 + 0.016\text{OCR} - 0.87\Delta I_{vy}\right]\text{OCR}^{0.42}\left(\max\left[\frac{h}{R}\ ;\ 8\right]\right)^{-0.20} \tag{5}$$

$$\Delta I_{vy} = \log_{10} S_t = \log_{10}\left(s_u / s_{ur}\right) \tag{6}$$

for the ICPDM, and

$$\sigma'_{hds} = \frac{0.23q_t\left[\max\left(\frac{h}{R}\ ;\ 1\right)\right]^{-0.2}}{\left(q_t/\sigma'_{v0}\right)^{0.15}} \tag{7}$$

for the UWAPDM, where q_t = corrected, total cone resistance [= q_c + (1 – a)u_2], q_c = measured cone resistance, a = cone area ratio (≈ 0.8 for typical CPT probes), u_2 = pore water pressure measured at the shoulder position behind the cone face, σ'_{v0} = initial vertical effective stress at the depth being considered, h = vertical distance from the pile base to the depth being considered, R = pile radius, OCR = overconsolidation ratio, S_t = sensitivity, and s_u and s_{ur} = *in situ* and remolded undrained shear strengths. In the absence of soil samples or laboratory test results, the values of OCR and s_u may be estimated from CPT data (Dagger et al. 2018; Mayne and Peuchen 2018). Both the ICPDM and the UWAPDM predict the value of q_{sL} after dissipation of the excess pore water pressure generated by pile installation. For open-ended pipe (OEP) piles, the use of an equivalent pile radius [= $(R^2 - R_i^2)^{0.5}$] has been suggested for estimation of q_{sL}, where R_i = inner radius of an OEP pile.

According to the ICPDM, the residual interface friction angle δ_r should be determined from the results of site-specific ring shear interface tests performed for the applicable value of normal effective stress (Ramsey et al. 1998). If such test results are unavailable, it is possible to estimate δ_r by recognizing that it varies with the normal effective stress σ' acting on the pile shaft. We discuss the residual shear strength of clay and its implications for pile design in section 3 of the paper. Because of the uncertainty associated with the value of δ_r for several of the test piles in the UWA database, the UWAPDM provides another equation to estimate the value of q_{sL} without the tan δ_r term (Lehane et al. 2013):

$$q_{sL} = 0.055q_t\left[\max\left(\frac{h}{R}\ ;\ 1\right)\right]^{-0.2} \tag{8}$$

In addition to the ICPDM and the UWAPDM, other modern pile design methods available in the literature for estimation of q_{sL} of driven piles in clay include the Unified Pile Design Method (UPDM) and the Purdue Pile Design Method (PPDM). According to the UPDM, the limit unit shaft resistance of an axially loaded driven pile in clay is given by (Lehane et al. 2022a, 2022b):

$$q_{sL} = 0.07F_{st}q_t\left[\max\left(\frac{h}{B}\ ;\ 1\right)\right]^{-0.25} \tag{9}$$

where F_{st} = sensitivity factor [= 1 for clays with $I_{z1} > 0$ in zones 2, 3, and 4 of the soil behavior type (SBT) chart ($I_c \geq 2.6$) (see Robertson 2009) and 0.5 ± 0.2 for clays with $I_{z1} < 0$ in zone 1 of the SBT chart], $I_{z1} = Q_{tn} - 12e^{-1.4F_r}$, Q_{tn} and F_r = normalized cone resistance and friction ratio (Robertson 2009), and B = pile diameter [= $(B^2 - B_i^2)^{0.5}$ for OEP piles; B_i = inner diameter of an OEP pile]. The UPDM predicts the value of q_{sL} after 80% dissipation of the excess pore pressure generated by pile installation.

According to the PPDM, the limit unit shaft resistance of an axially loaded driven pile in clay is given by (Basu et al. 2014; Salgado 2022):

$$q_{sL} = \alpha s_u \tag{10}$$

$$\alpha = 1.28\left(\frac{s_u}{\sigma'_{v0}}\right)^{-0.05}\left\{A_1 + (1 - A_1)\exp\left[-\left(\frac{\sigma'_{v0}}{p_A}\right)\left(\phi_c - \phi_{r,\min}\right)^{A_2}\right]\right\} \tag{11}$$

where A_1 = 0.75 for $\phi_c - \phi_{r,\min} \leq 5°$, 0.43 for $\phi_c - \phi_{r,\min} \geq 12°$, and a linearly interpolated value for $5° < \phi_c - \phi_{r,\min} < 12°$; A_2 = 0.64+0.4ln(s_u/σ'_{v0}); and $\phi_{r,\min}$ = minimum residual friction angle. The above PPDM equations predict the value of q_{sL} after full dissipation of the excess pore water pressure generated by pile installation.

2. Critical-state friction angle of sand

The critical-state friction angle ϕ_c is simply the friction angle that a given soil has at critical state. It is independent of soil state (i.e., relative density and confining stress) but depends on particle size (e.g., D_{50}), particle morphology (e.g., particle roundness and sphericity), mineralogy (e.g., silicates versus carbonates), and gradation (e.g., coefficient of uniformity) (Han et al. 2018; Salgado 2022). The value of ϕ_c for a silica sand typically ranges from 28° to 36°; sands with rounded, smooth particles with a poorly graded particle size distribution have values near the low end of this range, while sands with angular, rough particles with a well-graded particle size distribution have values near the high end of this range (Salgado 2022). In contrast, the value of ϕ_c for a carbonate sand typically ranges from 37° to 44° (Altuhafi et al. 2016; Coop and Lee 1993; Salgado 2022).

2.1. Data for silica sands

Table 1 summarizes the intrinsic parameters of 23 clean silica sands reported in the literature. The parameters include mean particle size D_{50}, coefficient of uniformity C_U, roundness R, sphericity S, minimum void ratio e_{min}, maximum void ratio e_{max}, and critical-state friction angle ϕ_c in triaxial compression. All the sands are poorly graded, except FS Ohio SW, which is classified as well-graded according to the Unified Soil Classification System (USCS) (ASTM D2487). The number designations for some of the uniform sands (e.g., Ottawa 20–30) listed in Table 1 indicate the sieve numbers between which the sand particles were retained. The D_{50}, C_U, and R values for the sands are in the range of 0.15–2.68 mm, 1.2–7.9, and 0.3–0.8, respectively. Although particle sphericity has been defined differently for some of the sands listed in Table 1, the S values lie within a relatively narrow range of 0.65–0.90, regardless of the definition used. Zheng and Hryciw (2016) also found the values of particle sphericity to lie within a similar range for the sands considered in their database. They reasoned that sand particles are usually bulky in nature and that slender, elongated sand particles are rarely found in practice because such particles are susceptible to breakage.

2.2. Simple correlation

In the absence of direct shear (DS) or triaxial compression (TXC) test results, a simple approach to critical-state friction angle estimation is to use an equation of the form:

$$\phi_c = C_1 \left(\frac{D_{50}}{D_{\text{ref}}} \right)^{C_2} \left(C_U \right)^{C_3} \left(R \right)^{C_4} \tag{12}$$

where D_{ref} = reference particle size (= 1 mm or 0.04 in.); and C_1, C_2, C_3, and C_4 = regression coefficients. The values of C_1, C_2, C_3, and C_4 were obtained by performing a least squares regression in Microsoft Excel. The following equation was found to fit the ϕ_c values reported in Table 1 quite well:

$$\phi_c \left(^\circ \right) = 28.3 \left(\frac{D_{50}}{D_{\text{ref}}} \right)^{\zeta} \left(C_U \right)^{2\zeta} \left(R \right)^{-3\zeta} \tag{13}$$

where ϕ_c = critical-state friction angle in triaxial compression, and ζ = exponent (= 0.045). The adjusted coefficient of determination r^2, mean absolute error, and mean absolute percentage error are 0.89, 0.4°, and 1.3%, respectively. The adjusted r^2 is a modified version of r^2 that has been adjusted for the number of independent variables considered in the model. Equation (13) is applicable for poorly graded, clean silica sands with D_{50} = 0.15–2.68 mm, C_U = 1.2–3.1, and R = 0.3–0.8; however, it should be used with caution for (a) well-graded sands with $C_U \geq 6$, (b) sands with D_{50}, C_U and R values that lie outside these ranges, and (c) sands with plastic or non-plastic fines greater than 5%.

Fig. 1 compares the critical-state friction angle predicted using Eq. (13) with that obtained from TXC test results for the poorly graded, clean silica sands listed in Table 1. The differences between the predicted and measured ϕ_c values are within 1°. To evaluate the performance of Eq. (13) in an unbiased manner, we considered two additional, poorly graded, clean silica sands: Nerlerk sand and Fujian sand; these sands were not used in the development of Eq. (13). The properties of Nerlerk sand are: D_{50} = 0.23 mm, C_U = 1.56, R = 0.43, S_{WL} = 0.75, e_{min} = 0.66, e_{max} = 0.89, and ϕ_c = 30° in triaxial compression (Sladen et al. 1985); the values of R and S_{WL} are based on Krumbein and Sloss (1951). The properties of Fujian sand are: D_{50} = 0.40 mm, C_U = 1.53, R = 0.55, and ϕ_c = 30.8° in triaxial compression (Yang and Wei 2012). The critical-state friction angle of Nerlerk sand and Fujian sand calculated using Eq. (13) is equal to 30.9° and 30.6°, respectively. Thus, the difference between the predicted and measured ϕ_c value is equal to 0.9° for Nerlerk sand and 0.2° for Fujian sand.

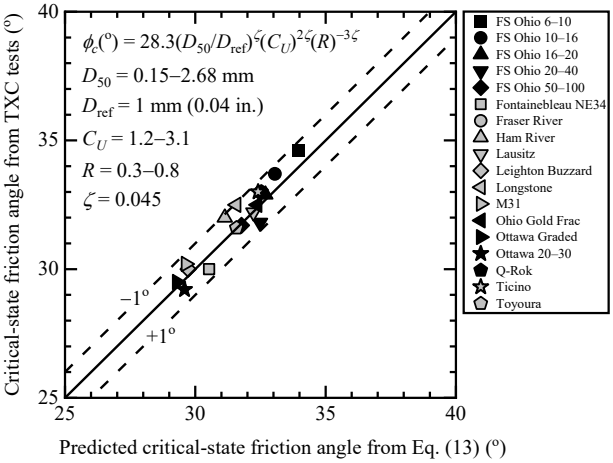

Figure 1. Comparison of ϕ_c values obtained from Eq. (13) and TXC tests on poorly graded, clean silica sands.

3. Residual friction angle of clay

The residual shear strength τ_r of clay is the product of the normal effective stress σ' on the shearing plane and the tangent of the residual friction angle ϕ_r, which, in turn, depends on the value of σ', the clay mineralogy, the clay fraction (CF), and the magnitude and rate of shear displacement. According to Skempton (1985), the shear displacements needed for an intact clay with CF > 30% and σ' < 600 kPa to attain residual friction angles of ϕ_r and ϕ_r + 1° range from 100–500 mm and 30–200 mm, respectively.

3.1. Effect of clay fraction

Depending on the clay fraction of the soil, different residual-state shearing mechanisms are possible, resulting in different values of ϕ_r (Lupini et al. 1981). Based on Skempton's observations on the variation of ϕ_r with the clay fraction of sand-bentonite mixtures tested in ring shear, Salgado (2006) proposed the following equation for ϕ_r of clay-silt-sand mixtures as a function of the clay fraction for a given stress level:

$$\phi_r = \phi_r\big|_{\text{pure clay}} + \left(\frac{\phi_{c,\text{mix}} - \phi_r\big|_{\text{pure clay}}}{27\%} \right) \left[52\% - \text{CF}(\%) \right] \tag{14}$$

where $\phi_{c,mix}$ = critical-state friction angle of the clay-silt-sand mixture, and $\phi_r|_{pure\ clay}$ = residual friction angle of the clay fraction of the mixture.

Table 1. Intrinsic parameters of 23 clean silica sands reported in the literature

Sand	Size and gradation		Morphology		Packing		Strength	Reference
	D_{50} (mm)	C_U	R	S	e_{min}	e_{max}	ϕ_c (°)	
FS Ohio 6–10	2.68	1.31	0.43	0.86	0.66	0.92	34.6	Han et al. (2018)
FS Ohio 10–16	1.59	1.30	0.44	0.83	0.65	0.92	33.7	Han et al. (2018)
FS Ohio 16–20	1.01	1.25	0.40	0.78	0.66	0.97	32.9	Han et al. (2018)
FS Ohio 20–40	0.63	1.42	0.39	0.82	0.62	0.91	31.8	Han et al. (2018)
FS Ohio 50–100	0.23	1.56	0.35	0.82	0.63	0.93	31.7	Han et al. (2018)
FS Ohio Coarse	1.50	2.00	—	—	0.45	0.72	33.6	Han et al. (2018)
FS Ohio Fine	0.35	2.00	—	—	0.48	0.72	33.4	Han et al. (2018)
FS Ohio SW	1.04	7.90	—	—	0.37	0.65	33.2[a]	Han et al. (2018)
Fontainebleau NE34	0.21	1.53	0.45	0.75[b]	0.51	0.90	30.0	Yang et al. (2010); Zheng and Hryciw (2016); Altuhafi et al. (2018)
Fraser River	0.30	2.40	0.43	0.83	0.68	1.00	33.0	Uthayakumar and Vaid (1998); Sukumaran and Ashmawy (2001); Gao et al. (2014)
Ham River	0.30	1.59	0.45	0.65[b]	0.59	0.92	32.0	Coop and Lee (1993); Jovicic and Coop (1997); Zheng and Hryciw (2016)
Lausitz	0.25	3.09	0.51	—	0.44	0.85	32.2	Herle and Gudehus (1999); Zheng and Hryciw (2016)
Leighton Buzzard	0.78	1.27	0.75	0.80[b]	0.51	0.80	30.0	Thurairajah (1962); Lings and Dietz (2004); Zheng and Hryciw (2016)
Longstone	0.15	1.43	0.30	0.65[b]	0.61	1.00	32.5	Tsomokos and Georgiannou (2010); Zheng and Hryciw (2016)
M31	0.28	1.54	0.62	0.70[b]	0.53	0.87	30.2	Tsomokos and Georgiannou (2010); Zheng and Hryciw (2016)
Monterey No. 0	0.38	1.58	—	0.89[c]	0.53	0.86	32.8	Riemer et al. (1990); Altuhafi et al. (2013)
Ohio Gold Frac	0.62	1.60	0.43	0.83	0.58	0.87	32.5	Han et al. (2018); Ganju et al. (2020)
Ottawa Graded	0.31	1.89	0.80[d]	0.90[d]	0.49	0.76	29.5	Carraro et al. (2009)
Ottawa 20–30	0.72	1.18	0.72	0.88	0.50	0.74	29.2	Han et al. (2018)
Q-Rok[d]	0.63	1.50	0.40	0.73	0.70	1.03	33.0	Unpublished research
Sacramento River	0.30	1.80	—	0.88[c]	0.53	0.87	33.2	Riemer et al. (1990); Altuhafi et al. (2013)
Ticino	0.58	1.50	0.40	0.80[b]	0.57	0.93	33.0	Bellotti et al. (1996); Cho et al. (2006); Altuhafi et al. (2016)
Toyoura	0.17	1.70	0.35	0.65[b]	0.60	0.98	31.6	Verdugo and Ishihara (1996); Loukidis and Salgado (2009); Zheng and Hryciw (2016)

Note: D_{50} = mean particle size, C_U = coefficient of uniformity (= D_{60}/D_{10}), e_{min} = minimum void ratio, e_{max} = maximum void ratio, R = particle roundness (Wadell 1932), S = diameter sphericity S_D (unless otherwise indicated) (Wadell 1933), and ϕ_c = critical-state friction angle in triaxial compression (unless otherwise indicated).

[a] Obtained from direct shear test results.

[b] Width-to-length ratio sphericity S_{WL} (Mitchell and Soga 2005; Zheng and Hryciw 2015).

[c] Perimeter sphericity S_P (Altuhafi et al. 2013).

[d] Unpublished research.

Table 2. Critical-state and residual friction angles of clayey soils reported in the literature

Soil	Mineralogy	CF (%)	PI (%)	A	ϕ_c (°)	$\phi_{r,\min}$ (°)	Reference
BBC	Illite, quartz	35	13.1	0.37	32.4[a]	—	Ladd and Varallyay (1965)
LC	Kaolinite, illite, montmorillonite, quartz	53–62	42–45	0.73–0.79	21.3	9.4[b]	Bishop et al. (1971); Gasparre (2005); Nishimura (2006)
LCT	Illite, calcite, quartz	14–20	10–12	0.60–0.71	30.0	—	Lupini et al. (1981); Gens (1982); Dafalias et al. (2006)
SFBM	Illite, montmorillonite	47	47	1.00	28.9[a]	16.2	Kirkgard and Lade (1991); Meehan (2006)
WC	Illite, kaolinite, illite-montmorillonite, vermiculite	52	33	0.63	20.9	8.3[c]	Parry (1960); Bishop et al. (1971); Akinlotan (2017)

Note: BBC = Boston Blue Clay, LC = London Clay, LCT = Lower Cromer Till, SFBM = San Francisco Bay Mud, WC = Weald Clay, CF = clay fraction, PI = plasticity index, A = activity (= PI/CF), ϕ_c = critical-state friction angle in triaxial compression, and $\phi_{r,\min}$ = minimum residual friction angle in ring shear.
[a] Extrapolated value corresponding to 30% axial strain (Chakraborty 2009).
[b] Value corresponds to blue London clay at Wraysbury (CF = 57%, PI = 43%, A = 0.75). For brown London clay at Walthamstow (CF = 53%, PI = 42%, A = 0.79), $\phi_{r,\min}$ = 7.5° (Bishop et al. 1971).
[c] Obtained from the fit of Eq. (15) to ring shear test data reported by Bishop et al. (1971).

For CF ≤ 25%, the bulky sand/silt particles are likely to control the behavior of the mixture and thus $\phi_r = \phi_{c,\text{mix}}$, whereas for CF ≥ 52%, the platy/tube-like/needle-like clay particles are likely to control the behavior of the mixture and thus $\phi_r = \phi_r|_{\text{pure clay}} \approx 5°$, 10°, and 15° for montmorillonite, illite, and kaolinite clay minerals, respectively (Skempton 1985). For intermediate values of CF between 25% and 52%, ϕ_r lies between $\phi_{c,\text{mix}}$ and $\phi_r|_{\text{pure clay}}$.

3.2. Effect of stress level

Besides the clay fraction and mineralogy, the residual friction angle ϕ_r also depends on the magnitude of the normal effective stress σ' acting on the shearing plane. ϕ_r decreases nonlinearly with increasing σ' because a larger normal stress forces greater realignment of clay particles in the direction of shearing. Soils with high clay fraction and high smectite content exhibit a significant drop in ϕ_r with increasing values of σ', while soils with low clay fraction and low smectite content may not exhibit any residual behavior. Following the work by Maksimović (1989), ϕ_r can be expressed as a function of σ' using (Salgado 2006):

$$\phi_r = \phi_{r,\min} + \frac{\phi_c - \phi_{r,\min}}{1 + \dfrac{\sigma'}{\sigma'_{\text{median}}}} \tag{15}$$

where σ' = normal effective stress on the plane of shearing, $\phi_{r,\min}$ = minimum residual friction angle (attained at large normal effective stress), ϕ_c = critical-state friction angle, and σ'_{median} = value of σ' at which the friction angle is equal to the average of $\phi_{r,\min}$ and ϕ_c.

According to the data compiled by Maksimović (1989), the value of σ'_{median} is in the range of 20–150 kPa depending on the clay type and mineralogy. At very large stresses, ϕ_r reaches an absolute minimum, denoted by $\phi_{r,\min}$. For σ' on the shearing plane approaching zero, ϕ_r approaches the critical-state friction angle ϕ_c due to the negligible reorientation of the clay particles in the absence of a normal stress forcing this reorientation to happen.

3.3. Data for some well-known clays

Table 2 summarizes the values of CF, PI, ϕ_c, and $\phi_{r,\min}$ for some well-known clayey soils reported in the literature. Although Lower Cromer till is a glacial till composed of sand (> 50%), clay (= 14–20%), and almost no silt (Gens 1982), it has been considered in the literature to behave like a "clay" but with no residual behavior. Boston blue clay is a low-plasticity, insensitive, marine clay, composed of illite and quartz (Terzaghi et al. 1996), and does not exhibit any residual behavior either (Ladd and Edgers 1972). San Francisco bay mud is a highly plastic silt containing a large amount of clay-size particles (montmorillonite and illite), organic substances, shell fragments, and traces of sand (Bonaparte 1982). London clay is composed of illite, kaolinite, montmorillonite, and quartz (Gasparre 2005); both San Francisco bay mud and London clay exhibit residual strength with sustained shearing beyond the critical state.

Fig. 2 illustrates the fit of Eq. (15) to ring shear test data for Weald clay. The fit is done by first estimating the value of ϕ_c from the triaxial compression test data of Parry (1960) and then finding the values of σ'_{median} and $\phi_{r,\min}$ that minimize the sum of least squares. The corresponding values of ϕ_c, $\phi_{r,\min}$, and σ'_{median} are 20.9°, 8.3°, and 51 kPa, respectively. The difference between the values of ϕ_c and $\phi_{r,\min}$ is equal to 12.6°.

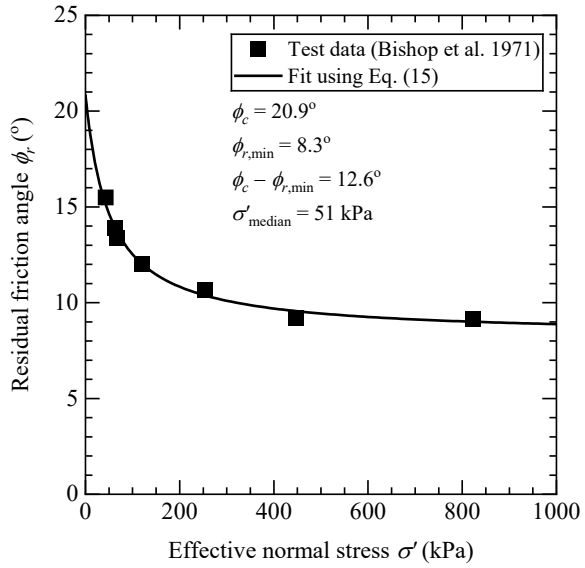

Figure 2. Fit of Eq. (15) to ring shear test data for Weald clay.

3.4. Implications for pile design

Both the ICPDM and the UWAPDM have expressions for q_{sL} that rely on the residual interface friction angle δ_r for the clay. In the absence of site-specific ring shear interface test results, it is possible to estimate δ_r by recognizing that it varies with the normal effective stress σ' on the pile operative at the time of shearing. Given that production piles are typically rough, we could take the value of δ_r at a given depth along the pile shaft to be approximately equal to that of the soil's residual friction angle ϕ_r at that depth. We can then use Eq. (15) to calculate δ_r along the pile shaft, with the value of σ' set equal to that of σ'_{hds} [given by Eqs. (4)–(6) for the ICPDM and by Eq. (7) for the UWAPDM].

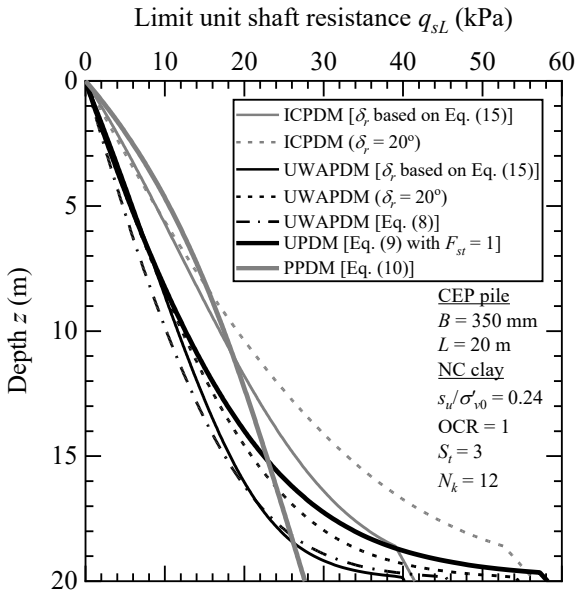

Figure 3. Comparison of q_{sL} profiles obtained using different pile design methods for a CEP pile in NC clay.

To illustrate the effect of δ_r on q_{sL}, we consider, for example, a 350-mm-diameter closed-ended pipe (CEP) pile driven to a depth of 20 m in normally consolidated (NC), saturated clay having the following properties: γ_{sat} = 18 kN/m^3, s_u/σ'_{v0} = 0.24, S_t = 3, ϕ_c = 24°, $\phi_{r,min}$ = 12°, and σ'_{median} = 50 kPa. The q_t profile is obtained through the relation: $q_t = s_u N_k + \sigma_{v0}$. Fig. 3 shows that, for both the ICPDM and UWAPDM, the values of q_{sL} estimated using a constant value for δ_r (e.g., 20°) are greater than those obtained considering the dependence of δ_r on σ' via Eq. (15); this trend is more significant in the lower half of the pile than the upper half of the pile. The ICPDM predicts values of Q_{sL} equal to 401 kN [for δ_r based on Eq. (15)] and 487 kN (for δ_r = 20°), whereas the UWAPDM predicts values of Q_{sL} equal to 282 kN and 320 kN, respectively, for these cases. Comparisons were also done using the UPDM and the PPDM; the corresponding values of Q_{sL} are 347 kN and 359 kN, respectively. These values lie within the range of Q_{sL} predictions obtained using the ICPDM and the UWAPDM.

4. SPT-CPT correlation

Fig. 4 shows a correlation between the CPT cone resistance q_c (or q_t in the case of clays) and the corrected SPT blow count N_{60} as a function of mean particle size D_{50}. The chart includes data reported by Robertson et al. (1983) and data collected from 15 sites in Indiana (2 sites each in Hamilton, Tippecanoe, Clinton and Greene Counties, and 1 site each in Jasper, Lake, Newton, Knox, Starke, Dubois and Carroll Counties). The following expression approximates the trend of the 98 data points plotted in Fig. 4:

$$\frac{q_c}{p_A N_{60}} = 6.95\left(\frac{D_{50}}{D_{ref}}\right)^{0.25} - 0.18 \quad \text{for } 0.001 \le \frac{D_{50}}{D_{ref}} \le 10 \quad (16)$$

where p_A = reference stress (= 100 kPa or 14.5 psi), D_{50} = mean particle size, and D_{ref} = reference particle size (= 1 mm or 0.04 in.). The coefficient of determination r^2 and the standard error of the regression are 0.89 and 0.77, respectively. Equation (16) may be used to obtain an estimate of q_c for use in a CPT-based foundation design method when only SPT blow counts are available for a site. However, as with any correlation involving the SPT blow count, Eq. (16) should be used with caution because of the potential error introduced by the transformation from the SPT blow count (a dynamic resistance) to the CPT cone resistance (a quasi-static resistance).

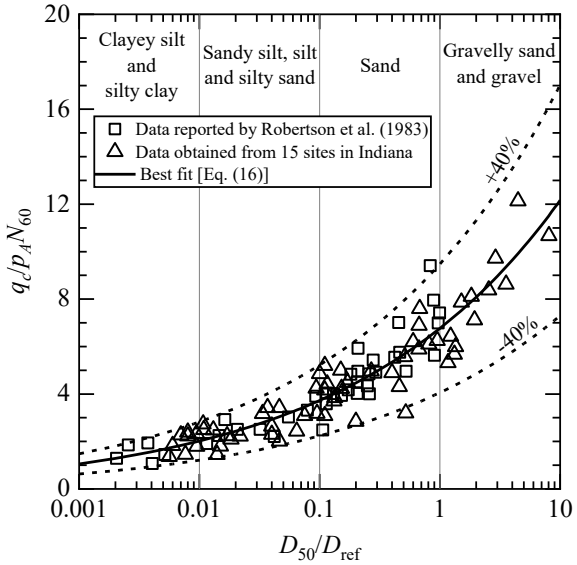

Figure 4. $q_c/p_A N_{60}$ versus D_{50}/D_{ref} for different soil types.

5. Conclusions

The design of pile foundations in sand and clay depends on certain key variables, such as the critical-state friction angle ϕ_c of sand and the residual friction angle ϕ_r of clay. A relationship between ϕ_c, mean particle size D_{50}, coefficient of uniformity C_U, and particle roundness R was developed using test data reported for poorly graded, clean silica sands in the literature. This relationship may be used to obtain an estimate of ϕ_c in the absence of direct shear or triaxial compression test results. For driven piles in clay, the limit unit shaft resistance of the pile is shown to depend on the pile-soil residual interface friction angle, which, in turn, depends on the normal effective stress on the pile operative at the time of shearing. Finally, a relationship between the cone resistance and the SPT blow count was developed using data collected from multiple sites in Indiana. The relationships proposed in this paper are restricted to the range of material properties and test conditions for which they were developed.

References

Akinlotan, O. "Mineralogy and palaeoenvironments: the Weald Basin (Early Cretaceous), Southeast England", Depos Rec, 3(2), pp. 187–200, 2017. https://doi.org/10.1002/dep2.32

Altuhafi, F., C. O'Sullivan, and I. Cavarretta "Analysis of an image-based method to quantify the size and shape of sand particles", J Geotech Geoenviron Eng, 139(8), pp. 1290–1307, 2013. https://doi.org/10.1061/(ASCE)GT.1943-5606.0000855

Altuhafi, F.N., M.R. Coop, and V.N. Georgiannou "Effect of particle shape on the mechanical behavior of natural sands", J Geotech Geoenviron Eng, 142(12), 04016071, 2016. https://doi.org/10.1061/(ASCE)GT.1943-5606.0001569

Altuhafi, F. N., R. J. Jardine, V. N. Georgiannou, and W. W. Moinet "Effects of particle breakage and stress reversal on the behaviour of sand around displacement piles", Géotechnique, 68(6), pp. 546–555, 2018. https://doi.org/10.1680/jgeot.17.P.117

American Society for Testing and Materials "ASTM D2487 Standard practice for classification of soils for engineering purposes (unified soil classification system)", ASTM International, West Conshohocken, PA, USA, 2017.

Basu, D., and R. Salgado "Load and resistance factor design of drilled shafts in sand", J Geotech Geoenviron Eng, 138(12), pp. 1455–1469, 2012.

Basu, P., M. Prezzi, R. Salgado, and T. Chakraborty. "Shaft resistance and setup factors for piles jacked in clay", J Geotech Geoenviron Eng, 140(3), 04013026, 2014. https://doi.org/10.1061/(ASCE)GT.1943-5606.0001018

Bellotti, R., M. Jamiolkowski, D. C. F. lo Presti, and D. A. O'Neill "Anisotropy of small strain stiffness in Ticino sand", Géotechnique, 46(1), pp. 115–131, 1996. https://doi.org/10.1680/geot.1996.46.1.115

Bishop, A. W., G. E. Green, V. K. Garga, A. Andresen, and J. D. Brown "A new ring shear apparatus and its application to the measurement of residual strength", Géotechnique, 21(4), pp. 273–328, 1971. https://doi.org/10.1680/geot.1971.21.4.273

Bonaparte, R. "A time-dependent constitutive model for cohesive soils", Doctoral, University of California, Berkeley, 1982.

Carraro, J. A. H., M. Prezzi, and R. Salgado "Shear strength and stiffness of sands containing plastic or nonplastic fines", J Geotech Geoenviron Eng, 135(9), pp. 1167–1178, 2009. https://doi.org/10.1061/(ASCE)1090-0241(2009)135:9(1167)

Chakraborty, T. "Development of a clay constitutive model and its application to pile boundary value problems", Doctoral, Purdue University, 2009. [online] Available at: [https://www.proquest.com/dissertations-theses/development-clay-constitutive-model-application/docview/304989818/se-2.

Cho, G.-C., J. Dodds, and J. C. Santamarina "Particle shape effects on packing density, stiffness, and strength: natural and crushed sands", J Geotech Geoenviron Eng, 132(5), pp. 591–602, 2006. https://doi.org/10.1061/(ASCE)1090-0241(2006)132:5(591)

Coop, M.R., and I.K. Lee "The behaviour of granular soils at elevated stresses", In: Predictive Soil Mechanics (Wroth Memorial Symposium), Oxford, UK, 1993, pp. 186–198.

Dafalias, Y. F., M. T. Manzari, and A. G. Papadimitriou "SANICLAY: simple anisotropic clay plasticity model", Int J Numer Anal Methods Geomech, 30(12), pp. 1231–1257, 2006. https://doi.org/10.1002/nag.524

Dagger, R., D. Saftner, and P. W. Mayne "Cone penetration test design guide for state geotechnical engineers", Minnesota Department of Transportation, St. Paul, MN, USA, Rep. MN/RC 2018-32, 2018.

Foye, K. C., G. Abou-Jaoude, M. Prezzi, and R. Salgado "Resistance factors for use in load and resistance factor design of driven pipe piles in sands", J Geotech Geoenviron Eng, 135(1), pp. 1–13, 2009. https://doi.org/10.1061/(ASCE)1090-0241(2009)135:1(1)

Ganju, E., F. Han, M. Prezzi, R. Salgado, and J. S. Pereira "Quantification of displacement and particle crushing around a penetrometer tip", Geosci Front, 11(2), pp. 389–399, 2020. https://doi.org/10.1016/j.gsf.2019.05.007

Gao, Z., J. Zhao, X.-S. Li, and Y. F. Dafalias "A critical state sand plasticity model accounting for fabric evolution", Int J Numer Anal Methods Geomech, 38(4), pp. 370–390, 2014. https://doi.org/10.1002/nag.2211

Gasparre, A. "Advanced laboratory characterization of London Clay", Doctoral, Imperial College London, 2005. [online] Available at: [http://hdl.handle.net/10044/1/45389].

Gens, A. "Stress–strain and strength of a low plasticity clay", Doctoral, Imperial College London, 1982. [online] Available at: [http://hdl.handle.net/10044/1/8410].

Han, F., R. Salgado, M. Prezzi, and J. Lim "Shaft and base resistance of non-displacement piles in sand", Comput Geotech, 83, pp. 184–197, 2017a.

Han, F., M. Prezzi, R. Salgado, and M. Zaheer "Axial resistance of closed-ended steel-pipe piles driven in multilayered soil", J Geotech Geoenviron Eng, 143(3), 04016102, 2017b. https://doi.org/10.1061/(ASCE)GT.1943-5606.0001589

Han, F., E. Ganju, R. Salgado, and M. Prezzi "Effects of interface roughness, particle geometry, and gradation on the sand-steel interface friction angle", J Geotech Geoenviron Eng, 144(12), 04018096, 2018.

Han, F., E. Ganju, R. Salgado, and M. Prezzi "Comparison of the load response of closed-ended and open-ended pipe piles driven in gravelly sand", Acta Geotech, 14, pp. 1785–1803, 2019. https://doi.org/10.1007/s11440-019-00863-1

Herle, I., and G. Gudehus "Determination of parameters of a hypoplastic constitutive model from properties of grain assemblies", Mech Cohes-Frict Mater, 4(5), pp. 461–486, 1999.

Jardine, R., F. Chow, R. Overy, and J. Standing "ICP design methods for driven piles in sands and clays", ICE Publishing (Thomas Telford Ltd), London, UK, 2005.

Jovicic, V., and M. R. Coop "Stiffness of coarse-grained soils at small strains", Géotechnique, 47(3), pp. 545–561, 1997. https://doi.org/10.1680/geot.1997.47.3.545

Kirkgard, M., and P. Lade "Anisotropy of normally consolidated San Francisco Bay Mud", Geotech Test J, 14(3), pp. 231–246, 1991. https://www.astm.org/gtj10568j.html

Krumbein, W. C., and L. L. Sloss "Stratigraphy and sedimentation", W. H. Freeman and Company, San Francisco, CA, USA, 1951.

Ladd, C. C., and J. Varallyay "The influence of the stress system on the behavior of saturated clays during undrained shear",

Massachusetts Institute of Technology, Cambridge, MA, USA, Rep. R65-11, 1965.
Ladd, C. C., and L. Edgers "Consolidated-undrained direct simple shear tests on Boston Blue Clay", Massachusetts Institute of Technology, Cambridge, USA, Rep. R72-82, 1972.
Lehane, B. M., Y. Li, and R. Williams "Shaft capacity of displacement piles in clay using the cone penetration test", J Geotech Geoenviron Eng, 139(2), pp. 253–266, 2013. https://doi.org/10.1061/(ASCE)GT.1943-5606.0000749
Lehane, B. M., Z. Liu, E. J. Bittar, F. Nadim, S. Lacasse, N. Bozorgzadeh, R. Jardine, J.-C. Ballard, P. Carotenuto, K. Gavin, R. B. Gilbert, J. Bergan-Haavik, P. Jeanjean, and N. Morgan. "CPT-based axial capacity design method for driven piles in clay", J Geotech Geoenviron Eng, 148(9), 04022069, 2022a.https://doi.org/10.1061/(ASCE)GT.1943-5606.0002847
Lehane, B. M., E. Bittar, S. Lacasse, Z. Liu, and F. Nadim. "New CPT methods for evaluation of the axial capacity of driven piles", In: Cone Penetration Testing 2022, 1st ed., CRC Press (Taylor & Francis Group), London, UK, 2022b, pp. 3–15.
Lings, M. L., and M. S. Dietz "An improved direct shear apparatus for sand", Géotechnique, 54(4), pp. 245–256, 2004. https://doi.org/10.1680/geot.2004.54.4.245
Loukidis, D., and R. Salgado "Analysis of the shaft resistance of non-displacement piles in sand", Géotechnique, 58(4), pp. 283–296, 2008.
Loukidis, D., and R. Salgado "Modeling sand response using two-surface plasticity", Comput Geotech, 36(1–2), pp. 166–186,2009. https://doi.org/10.1016/j.compgeo.2008.02.009
Lupini, J. F., A. E. Skinner, and P. R. Vaughan "The drained residual strength of cohesive soils", Géotechnique, 31(2), pp. 181–213, 1981. https://doi.org/10.1680/geot.1981.31.2.181
Maksimović, M. "On the residual shearing strength of clays", Géotechnique, 39(2), pp. 347–351, 1989. https://doi.org/10.1680/geot.1989.39.2.347
Mayne, P. W., and J. Peuchen "Evaluation of CPTU N_{kt} cone factor for undrained strength of clays", In: Cone Penetration Testing 2018, 1st ed., Taylor & Francis Group, Oxfordshire, UK, 2018, pp. 423–429.
Meehan, C. L. "An experimental study of the dynamic behavior of slickensided surfaces", Doctoral, Virginia Polytechnic Institute and State University, 2006. [online] Available at: [http://hdl.handle.net/10919/26074].
Mitchell, J. K., and K. Soga "Fundamentals of soil behavior", 3rd ed., John Wiley & Sons, Inc., Hoboken, NJ, 2005.
Nishimura, S. "Laboratory study on anisotropy of natural London clay", Doctoral, Imperial College London, 2006.
Parry, R. H. G. "Triaxial compression and extension tests on remoulded saturated clay", Géotechnique, 10(4), pp. 166–180, 1960. https://doi.org/10.1680/geot.1960.10.4.166
Ramsey, N., R. Jardine, B. Lehane, and A. Ridley "A review of soil-steel interface testing with the ring shear apparatus", In: Offshore Site Investigation and Foundation Behaviour (New Frontiers), London, UK, 1998, pp. 237–258.
Riemer, M. F., R. B. Seed, P. G. Nicholson, and H. -L. Jong "Steady state testing of loose sands: limiting minimum density", J Geotech Eng, 116(2), pp. 332–337, 1990. https://doi.org/10.1061/(ASCE)0733-9410(1990)116:2(332)
Robertson, P. K., R. G. Campanella, and A. Wightman "SPT-CPT correlations", J Geotech Eng, 109(11), pp. 1449–1459, 1983.
Robertson, P. K. "Interpretation of cone penetration tests — a unified approach", Can Geotech J, 46(11), pp. 1337–1355, 2009. https://doi.org/10.1139/T09-065
Sakleshpur, V. A., M. Prezzi, R. Salgado, and M. Zaheer "CPT-based geotechnical design manual, Volume 2: CPT-based design of foundations (methods)", Joint Transportation Research Program, West Lafayette, IN, USA, Rep. FHWA/IN/JTRP-2021/23, 2021a.
Sakleshpur, V. A., M. Prezzi, R. Salgado, and M. Zaheer "CPT-based geotechnical design manual, Volume 3: CPT-based design of foundations (example problems)", Joint Transportation Research Program, West Lafayette, IN, USA, Rep. FHWA/IN/JTRP-2021/24, 2021b.
Salgado, R. "The role of analysis in non-displacement pile design", In: Modern Trends in Geomechanics, Springer Proceedings in Physics (Volume 106), Springer, Berlin, Heidelberg, 2006, pp. 521–540. https://doi.org/10.1007/978-3-540-35724-7_30
Salgado, R., and M. Prezzi "Computation of cavity expansion pressure and penetration resistance in sands", Int J Geomech, 7(4), pp. 251–265, 2007.
Salgado, R. "The engineering of foundations, slopes and retaining structures", 2nd ed., CRC Press, Boca Raton, FL, 2022. https://doi.org/10.1201/b22079
Skempton, A. W. "Residual strength of clays in landslides, folded strata and the laboratory", Géotechnique, 35(1), pp. 3–18, 1985. https://doi.org/10.1680/geot.1985.35.1.3
Sladen, J. A., R. D. D'Hollander, and J. Krahn "The liquefaction of sands, a collapse surface approach", Can Geotech J, 22(4), pp. 564–578, 1985. https://doi.org/10.1139/t85-076
Sukumaran, B., and A. K. Ashmawy "Quantitative characterisation of the geometry of discrete particles", Géotechnique, 51(7), pp. 619–627, 2001. https://doi.org/10.1680/geot.2001.51.7.619
Tehrani, F. S., F. Han, R. Salgado, M. Prezzi, R. D. Tovar, and A. G. Castro "Effect of surface roughness on the shaft resistance of non-displacement piles embedded in sand", Géotechnique, 66(5), pp. 386–400, 2016. https://doi.org/10.1680/jgeot.15.P.007
Terzaghi, K., R. B. Peck, and G. Mesri "Soil mechanics in engineering practice", 3rd ed., John Wiley & Sons, Inc., New York, USA, 1996.
Thurairajah, A. "Some shear properties of kaolin and of sand", Doctoral, University of Cambridge, 1962. https://doi.org/10.17863/CAM.31111
Tovar-Valencia, R. D., A. Galvis-Castro, R. Salgado, and M. Prezzi "Effect of surface roughness on the shaft resistance of displacement model piles in sand", J Geotech Geoenviron Eng, 144(3), 04017120, 2018.
Tsomokos, A., and V. N. Georgiannou "Effect of grain shape and angularity on the undrained response of fine sands", Can Geotech J, 47(5), pp. 539–551, 2010. https://doi.org/10.1139/T09-121
Uthayakumar, M., and Y. P. Vaid "Static liquefaction of sands under multiaxial loading", Can Geotech J, 35(2), pp. 273–283, 1998. https://doi.org/10.1139/t98-007
Verdugo, R., and K. Ishihara "The steady state of sandy soils", Soils Found, 36(2), pp. 81–91, 1996. https://doi.org/10.3208/sandf.36.2_81
Wadell, H. "Volume, shape, and roundness of rock particles", J Geol, 40(5), pp. 443–451, 1932.
Wadell, H. "Sphericity and roundness of rock particles", J Geol, 41(3), pp. 310–331, 1933.
Yang, Z. X., R. J. Jardine, B. T. Zhu, P. Foray, and C. H. C. Tsuha "Sand grain crushing and interface shearing during displacement pile installation in sand", Géotechnique, 60(6), pp. 469–482, 2010. https://doi.org/10.1680/geot.2010.60.6.469
Yang, J., and L. M. Wei "Collapse of loose sand with the addition of fines: the role of particle shape", Géotechnique, 62(12), pp. 1111–1125, 2012.
Zheng, J., and R. D. Hryciw "Traditional soil particle sphericity, roundness and surface roughness by computational geometry", Géotechnique, 65(6), pp. 494–506, 2015. https://doi.org/10.1680/geot.14.P.192
Zheng, J., and R. D. Hryciw "Index void ratios of sands from their intrinsic properties", J Geotech Geoenviron Eng, 142(12), 06016019, 2016.